

# An experimental compliance calibration strategy for estimating the elastic interface constants of delamination test specimens

Stefano Bennati<sup>1</sup>, Paolo S. Valvo<sup>1</sup>

<sup>1</sup>*Department of Civil and Industrial Engineering, University of Pisa, Italy*  
E-mail: s.bennati@ing.unipi.it, p.valvo@ing.unipi.it

*Keywords:* Fibre-reinforced laminates, Delamination, Interface models, Experimental testing.

**SUMMARY.** The delamination of composite laminates can be effectively modelled by considering a delaminated laminate as an assemblage of sublaminates connected by an elastic interlaminar interface. In this context, the question arises on the values to be assigned to the elastic interface constants. In the present study, we show how the elastic interface constants can be estimated through an experimental compliance calibration strategy. The method is based on the analytical solution for the MMB test, derived in a previous study. Here, a nonlinear least squares fitting procedure is applied to obtain the values of the elastic interface constants from the experimental results of DCB and ENF tests. Preliminary experimental tests have been conducted to check the effectiveness of the proposed strategy.

## 1 INTRODUCTION

Delamination is a typical failure mode affecting fibre-reinforced composite laminates [1]. The phenomenon is commonly modelled in the context of Fracture Mechanics. Consistently, a delamination crack is expected to propagate when the associated *energy release rate*,  $G$ , attains a critical value, or *fracture toughness*,  $G_c$  [2]. In general,  $G$  is the sum of three contributions,  $G_I$ ,  $G_{II}$ , and  $G_{III}$ , respectively related to fracture modes I (opening), II (sliding), and III (tearing). Since for anisotropic materials – such as composite laminates – the delamination toughness may depend strongly on fracture modes, specific laboratory tests are used to determine the critical values of  $G$  in fracture modes I, II, III, and combinations thereof [3].

The *mixed-mode bending* (MMB) test is the ASTM standard test procedure to determine the delamination toughness of laminated specimens under I/II mixed mode fracture conditions [4]. Actually, the MMB test can be regarded as the superposition of the *double cantilever beam* (DCB) and *end notched flexure* (ENF) tests, respectively used for pure fracture modes I and II [5, 6].

An effective modelling approach considers a delaminated laminate as an assemblage of sublaminates connected by a deformable interlaminar interface. In the simplest formulation, the interface consists of a continuous distribution of linearly elastic springs acting in the directions normal and tangential to the interface plane [7]. We have exploited this modelling technique to develop an *enhanced beam-theory* (EBT) model of the *asymmetric double cantilever beam* (ADCB) test, for which a numerical-analytical solution strategy has been proposed [8]. Recently, we have developed an EBT model of the MMB test and obtained a complete analytical solution [9], which includes also, as special cases, the solutions for the DCB and ENF tests. In particular, we have determined explicit expressions for the main quantities of interest, such as the specimen's compliance, energy release rate, and mode mixity [10].

As a matter of fact, the predictive effectiveness of the aforementioned models rests on the reliable estimation of the values of the *elastic interface constants*,  $k_z$  and  $k_x$ , respectively corresponding to the normal and tangential distributed springs. In the present study, we show how

the elastic interface constants can be estimated through an experimental compliance calibration strategy. The method is based on the observation that – according to the EBT model – the compliance of a DCB test specimen,  $C_{\text{DCB}}$ , depends on the normal springs elastic constant,  $k_z$ , and not on  $k_x$ . *Vice versa*, the compliance of an ENF test specimen,  $C_{\text{ENF}}$ , depends on the tangential springs elastic constant,  $k_x$ , and not on  $k_z$ . Therefore, the values of  $k_z$  and  $k_x$  can be traced from the experimental measurements of  $C_{\text{DCB}}$  and  $C_{\text{ENF}}$ , respectively.

The strategy is implemented for the MMB test as follows. Before carrying out the MMB tests at the desired levels of mode mixity, preliminary DCB and ENF tests are conducted on the same lot of specimens. Such tests are aimed at obtaining not only the measures of delamination toughness in pure fracture modes I and II, but also the experimental values of compliance. As a result, values of  $C_{\text{DCB}}$  and  $C_{\text{ENF}}$  as functions of the delamination length,  $a$ , are obtained. A nonlinear least squares fitting procedure is then applied to determine the optimal values of the elastic interface constants.

In order to illustrate the method, a set of unidirectional laminated specimens has been obtained from a typical carbon fibre/epoxy matrix composite laminate. DCB and ENF tests have been conducted and the compliance calibration strategy has been applied, providing a first, but significant, confirmation of its effectiveness.

## 2 THE EBT MODEL OF THE MMB TEST

### 2.1 *Experimental procedure and mechanical model*

We consider a laminated specimen (Fig. 1b) of length  $L$ , width  $B$  (not shown in the figure), and thickness  $H = 2h$ . The specimen is split by a delamination of length  $a$  into two sublaminates having identical mechanical properties. In the MMB test, the specimen is simply supported and loaded indirectly through a rigid lever (Fig. 1a). The load applied by the testing machine,  $P$ , is transferred to the specimen as an upward load,  $P_u$ , and a downward load,  $P_d$ . The lever arm lengths,  $c$  and  $d$ , can be adjusted to vary the intensities of  $P_u$  and  $P_d$  and, consequently, impose a desired I/II mixed-mode ratio,  $\alpha = G_I / G_{\text{II}}$ . For what follows, it is useful to define the lengths  $b = L - a$  and  $\ell = L - d$ . In conformity with the ASTM standard [4], the downward load,  $P_d$ , is applied at the specimen's mid-span section, so that  $\ell = d = L/2$ . Global reference  $x$ - and  $z$ -axes are fixed, aligned with the specimen's axial and transverse directions, respectively.

According to the enhanced beam-theory (EBT) model, the sublaminates may have any stacking sequences, provided that they behave as plane beams and exhibit neither shear-extension nor bending-extension coupling [9]. Incidentally, we note that this condition is fulfilled not only by homogenous and unidirectional laminated specimens, but also by symmetric cross-ply and angle-ply specimens, as well as other types of multidirectional laminated specimens [11]. In line with classical laminated plate theory [12], we denote with  $A_1 = A_2$ ,  $C_1 = C_2$ , and  $D_1 = D_2$  the sublaminates' extensional stiffness, shear stiffness, and bending stiffness, respectively. For homogeneous orthotropic specimens, by denoting  $E_x$ ,  $E_y$ ,  $E_z$  and  $G_{xy}$ ,  $G_{yz}$ ,  $G_{zx}$  as the elastic moduli in the fixed reference system, the sublaminates' stiffnesses are  $A_1 = E_x h$ ,  $C_1 = 5 G_{zx} h / 6$ , and  $D_1 = E_x h^3 / 12$ .

In the proposed model, the sublaminates are partly connected by a deformable interface, which is regarded as a continuous distribution of linearly elastic–brittle springs acting along the normal and tangential directions with respect to the interface plane. Correspondingly,  $k_z$  and  $k_x$  denote the elastic constants of the distributed springs (Fig. 1c).

In Ref. [9], the problem has been formulated using a set of differential equations based on

Timoshenko's beam theory and a complete explicit solution has been deduced, including analytical expressions for the internal forces, interfacial stresses, and displacements. In Ref. [10], analytical expressions for the specimen's compliance, energy release rate, and mode mixity have been deduced.

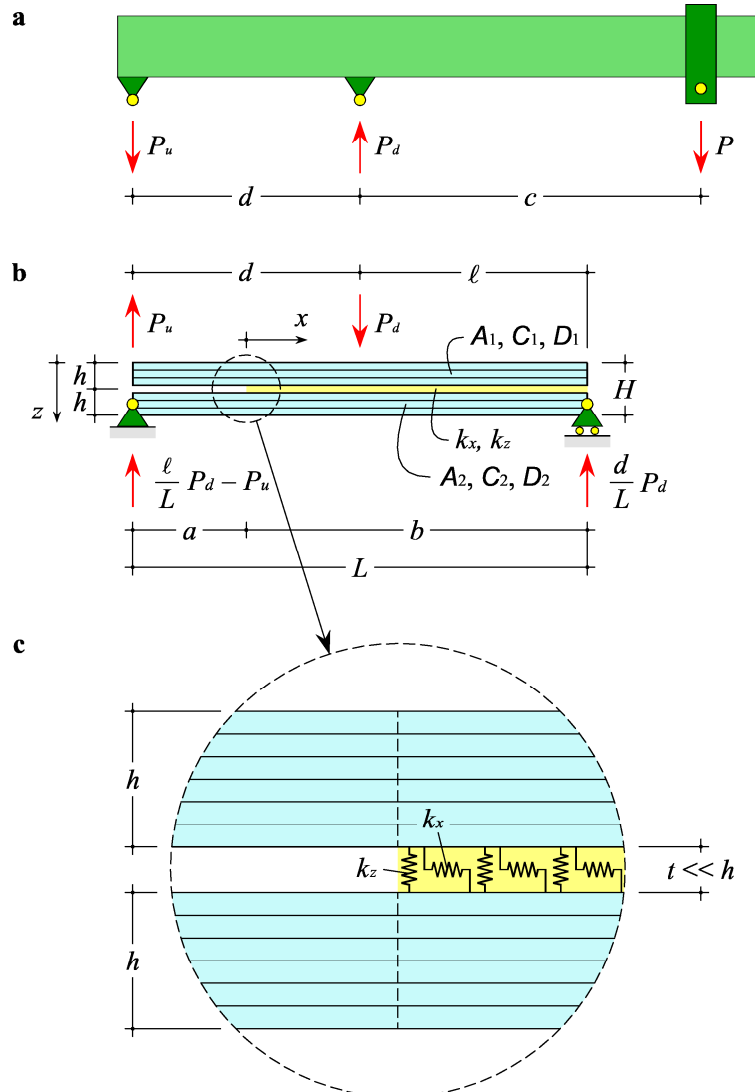


Figure 1: The MMB test: a) loading lever; b) enhanced beam-theory model; c) detail of the crack tip region and elastic interface.

## 2.2 Compliance

Assuming a linearly elastic load-deflection response, the specimen's compliance is generally defined as  $C = \delta / P$ , where  $P$  is the applied load and  $\delta$  is the displacement of the load application

point [2, 3]. According to the EBT model, the MMB test specimen's compliance turns out to be

$$C_{\text{MMB}} = \left(\frac{3c-\ell}{4\ell}\right)^2 C_{\text{DCB}} + \left(\frac{c+\ell}{\ell}\right)^2 C_{\text{ENF}}, \quad (1)$$

where

$$\begin{aligned} C_{\text{DCB}} &= \frac{2a^3}{3BD_1} + \frac{2a}{BC_1} + \frac{2}{\lambda_1\lambda_2BD_1} [(\lambda_1 + \lambda_2)a^2 + 2a + \frac{1}{\lambda_1} + \frac{1}{\lambda_2}] \quad \text{and} \\ C_{\text{ENF}} &= \frac{1}{24B} \frac{A_1h^2}{A_1h^2 + 4D_1} \left(\frac{a^3}{D_1} + \frac{8\ell^3}{A_1h^2}\right) + \frac{\ell}{4BC_1} + \\ &\quad + \frac{1}{8BD_1} \frac{A_1h^2}{A_1h^2 + 4D_1} \frac{1}{\lambda_5^2} [\lambda_5 a^2 + a + 2\ell - \frac{2}{\lambda_5} - \frac{4a}{\exp \lambda_5(\ell - a)}] \end{aligned} \quad (2)$$

are the compliances of the DCB and ENF test specimens, respectively. In Eqs. (2),

$$\lambda_1 = \sqrt{\frac{k_z}{C_1} \left(1 + \sqrt{1 - \frac{2C_1^2}{k_z D_1}}\right)}, \quad \lambda_2 = \sqrt{\frac{k_z}{C_1} \left(1 - \sqrt{1 - \frac{2C_1^2}{k_z D_1}}\right)}, \quad \text{and} \quad \lambda_5 = \sqrt{2k_x \left(\frac{1}{A_1} + \frac{h^2}{4D_1}\right)} \quad (3)$$

are the roots of the characteristic equations of the governing differential problem.

For orthotropic specimens, the above expressions become

$$\begin{aligned} C_{\text{DCB}} &= \frac{8a^3}{BE_x h^3} + \frac{12a}{5BG_{zx}h} + \frac{24}{BE_x h^3} \frac{1}{\lambda_1\lambda_2} [(\lambda_1 + \lambda_2)a^2 + 2a + \frac{1}{\lambda_1} + \frac{1}{\lambda_2}] \quad \text{and} \\ C_{\text{ENF}} &= \frac{3a^3 + 2\ell^3}{8BE_x h^3} + \frac{3\ell}{10BG_{zx}h} + \frac{9}{8BE_x h^3} \frac{1}{\lambda_5^2} [\lambda_5 a^2 + a + 2\ell - \frac{2}{\lambda_5} - \frac{4a}{\exp \lambda_5(\ell - a)}]. \end{aligned} \quad (4)$$

and

$$\lambda_1 = \sqrt{\frac{6}{5} \frac{k_z}{G_{zx}h} \left(1 + \sqrt{1 - \frac{50}{3} \frac{G_{zx}^2}{k_z E_x h}}\right)}, \quad \lambda_2 = \sqrt{\frac{6}{5} \frac{k_z}{G_{zx}h} \left(1 - \sqrt{1 - \frac{50}{3} \frac{G_{zx}^2}{k_z E_x h}}\right)}, \quad \text{and} \quad \lambda_5 = 2\sqrt{\frac{2k_x}{E_x h}}. \quad (5)$$

By inspection of Eqs. (2) and (4), we see that each of the quantities  $C_{\text{DCB}}$  and  $C_{\text{ENF}}$  is the sum of three contributions: the first addend depends on the sublaminates' bending stiffness and is the only term considered according to the simple beam-theory (SBT) model; the second addend is due to transverse shear deformability, in line with Timoshenko's beam theory; lastly, the third addend is due to the elastic interface deformability. Moreover, we observe that the compliances  $C_{\text{DCB}}$  and  $C_{\text{ENF}}$  are expressed by cubic polynomial functions of the delamination length,  $a$ , except for an exponential term (negligible in most cases) appearing in the expressions for  $C_{\text{ENF}}$ . Lastly, we note that the expressions for  $C_{\text{DCB}}$  depend on  $k_z$  (through  $\lambda_1$  and  $\lambda_2$ ) and not on  $k_x$  and, conversely, the expressions for  $C_{\text{ENF}}$  depend on  $k_x$  (through  $\lambda_5$ ) and not on  $k_z$ . Such last observations prepare the ground for the compliance calibration strategy, illustrated in what follows.

### 2.3 Energy release rate

The energy release rate of a cracked body is in general defined as  $G = -dV/dA$ , where  $V$  is the total potential energy and  $dA$  is the area of the new surface created by crack advancement [2, 3]. For a linearly elastic body of constant width  $B$ , the energy release rate can be obtained as

$$G = \frac{P^2}{2B} \frac{dC}{da}. \quad (6)$$

Under I/II mixed-mode fracture conditions,  $G = G_I + G_{II}$ , where  $G_I$  and  $G_{II}$  are the contributions related to fracture modes I and II, respectively. For a symmetric MMB test specimen, such contribution respectively correspond to

$$G_I = \frac{P_I^2}{2B} \frac{dC_{DCB}}{da} \quad \text{and} \quad G_{II} = \frac{P_{II}^2}{2B} \frac{dC_{ENF}}{da}, \quad (7)$$

where

$$P_I = \frac{1}{2} \left( \frac{c+d}{L} + \frac{c}{d} - 1 \right) P \quad \text{and} \quad P_{II} = \left( 1 + \frac{c}{d} \right) P \quad (8)$$

are the loads responsible for fracture modes I and II, respectively. By substituting Eqs. (2) into (7),

$$G_I = \frac{P_I^2}{B^2 D_1} (a + \chi_I h)^2 \quad \text{and} \quad G_{II} = \frac{P_{II}^2}{16B^2 D_1} \frac{A_1 h^2}{A_1 h^2 + 4D_1} (a + \chi_{II} h)^2, \quad (9)$$

where

$$\chi_I = \frac{1}{h} \left( \frac{1}{\lambda_1} + \frac{1}{\lambda_2} \right) = \frac{1}{h} \sqrt{\frac{D_1}{C_1} + \frac{2D_1}{k_z}} \quad \text{and} \quad \chi_{II} = \frac{1}{h} \frac{1}{\lambda_5} = \frac{1}{h} \frac{1}{\sqrt{2k_x \left( \frac{1}{A_1} + \frac{h^2}{4D_1} \right)}} \quad (10)$$

are *crack length correction parameters*, analogous to those introduced by the corrected beam-theory (CBT) model for orthotropic specimens [13, 14].

For orthotropic specimens, Eqs. (9) and (10) respectively reduce to

$$G_I = \frac{12P_I^2}{B^2 E_x h^3} (a + \chi_I h)^2 \quad \text{and} \quad G_{II} = \frac{9P_{II}^2}{16B^2 E_x h^3} (a + \chi_{II} h)^2 \quad (11)$$

and

$$\chi_I = \sqrt{\frac{E_x}{10G_{zx}} + \frac{E_x}{6k_z h}} \quad \text{and} \quad \chi_{II} = \sqrt{\frac{E_x}{8k_x h}}. \quad (12)$$

### 3 COMPLIANCE CALIBRATION STRATEGY

The proposed compliance calibration strategy requires that DCB and ENF tests are conducted on specimens obtained from the laminate under examination. As a result, the experimental values of the mode I compliance,  $C_{\text{DCB},i}$ , are obtained for a set of values of the delamination length,  $a_i$ , with  $i=1, 2, \dots, n$ . Likewise, the mode II compliance values,  $C_{\text{ENF},j}$ , are obtained for the delamination lengths,  $a_j$ , with  $j=1, 2, \dots, m$ .

In this regard, we note that while crack growth is stable in the DCB test, it is unstable in the ENF test. Consequently, the  $C_{\text{DCB},i}$  values can be recorded while monitoring the crack propagation during the test. Instead, the  $C_{\text{ENF},j}$  values must be obtained through a different strategy. For instance, they can be obtained by suitably shifting the specimen on the supporting rollers in order to change the position of the crack tip, hence the delamination length. For each position, the specimen is loaded within the elastic range (without crack propagation) and the corresponding values of compliance are recorded.

A nonlinear least squares fitting procedure is applied to determine the optimal values of the elastic interface constants. The sums of the squares of the residuals of the two sets of experimental data are

$$R_1^2 = \sum_{i=1}^n [C_{\text{DCB},i} - C_{\text{DCB}}(k_z)]^2 \quad \text{and} \quad R_2^2 = \sum_{j=1}^m [C_{\text{ENF},j} - C_{\text{ENF}}(k_x)]^2. \quad (13)$$

In order to minimise such sums, the following necessary conditions are imposed

$$\begin{aligned} \frac{d}{dk_z}(R_1^2) &= -2 \sum_{i=1}^n [C_{\text{DCB},i} - C_{\text{DCB}}(k_z)] \frac{dC_{\text{DCB}}}{dk_z} = 0 \quad \text{and} \\ \frac{d}{dk_x}(R_2^2) &= -2 \sum_{j=1}^m [C_{\text{ENF},j} - C_{\text{ENF}}(k_x)] \frac{dC_{\text{ENF}}}{dk_x} = 0. \end{aligned} \quad (14)$$

The derivatives of  $C_{\text{DCB}}$  and  $C_{\text{ENF}}$  have been calculated analytically from Eqs. (2) and (3), albeit their expressions are omitted here for the sake of conciseness. Eqs. (14) have then been solved numerically and the calibrated values of  $k_z$  and  $k_x$  finally obtained.

### 4 EXPERIMENTAL TESTS

In order to illustrate the method, experimental tests have been conducted on a set of unidirectional laminated specimens obtained from a typical carbon fibre/epoxy matrix composite laminate. The specimens have been produced and tested at the laboratory of the CETMA consortium in Brindisi.

Average material properties, determined through preliminary tests, are the following: longitudinal Young's modulus  $E_x = 116$  GPa, transverse shear modulus  $G_{zx} = 0.5$  GPa. Average dimensions of the specimens are  $B = 25.3$  mm,  $H = 2h = 2.8$  mm.

According to the AECMA standards [5, 6], DCB tests have been conducted first on 250 mm long specimens (Fig. 2a), until a total delamination length of about 100 mm had been achieved. Next, ENF tests have been conducted on the same specimens (Fig. 2b), after a residual part of the delaminated portion had been cut off.

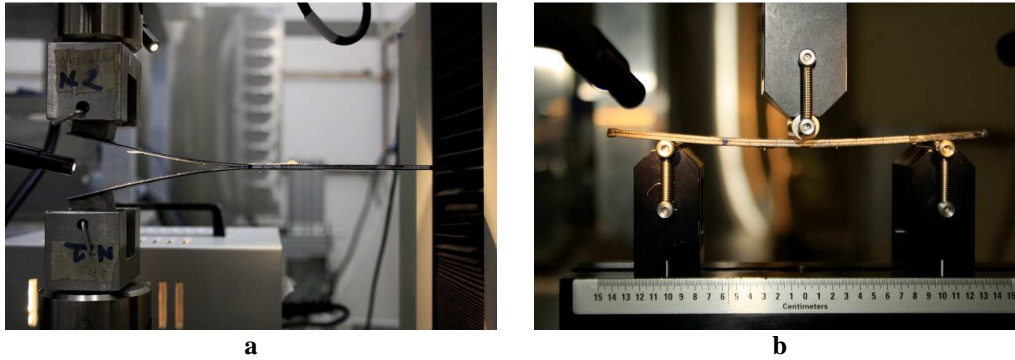


Figure 2: Delamination tests: a) DCB test; b) ENF test.

Figures 3a and 3b show the typical load-displacement plots obtained for the DCB and ENF tests, respectively. Please, notice that for the ENF test, several tests have been conducted within the elastic range of behaviour, at different values of the delamination length in order to obtain the corresponding values of compliance. For  $a = 20$  mm, the test has been carried out until the onset and growth of the delamination crack in order to determine the critical energy release rate.

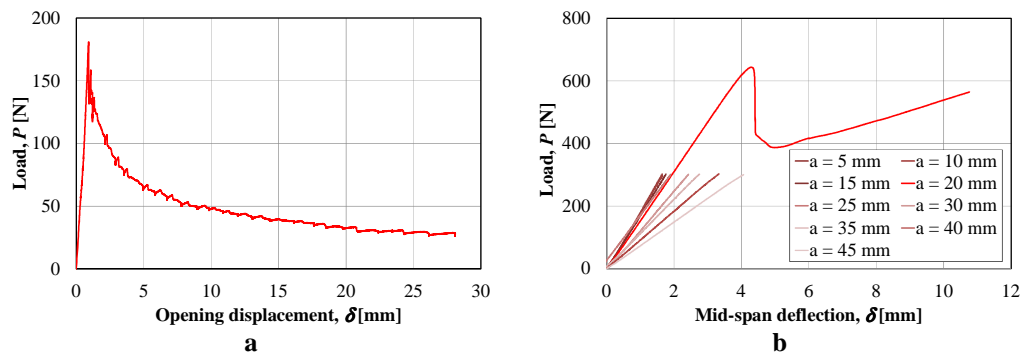


Figure 3: Applied load vs. displacement: a) DCB test; b) ENF test.

Figures 4a and 4b show the typical plots of compliance vs. delamination length obtained for the DCB and ENF tests, respectively. Black circles represent the experimental data. Dashed blue lines are the predictions of the SBT model, which, as known in the literature, underestimates the actual specimen's compliance. Continuous red lines are the predictions of the EBT model with the values of the elastic interface constants obtained as explained in Section 3 (see Table 1). Some discrepancies between the EBT model's predictions and experimental data are observed for larger values of delamination length. Such discrepancies can be probably explained by invoking the geometric nonlinearities occurring at the higher load and displacement values in the experimental tests, in particular the DCB test. Actually, such nonlinearities are completely neglected by the theoretical model. For this reason, when applying the nonlinear least squares fitting procedure to the mode I test results, only data corresponding to delamination lengths up to 50 mm have been considered.

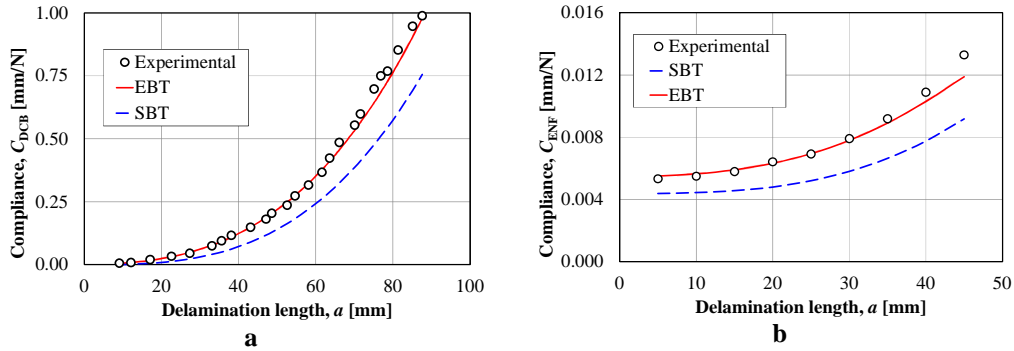


Figure 4: Compliance vs. delamination length: a) DCB test; b) ENF test.

Table 1: Elastic interface constants.

Specimen No.	Mode I $k_z$ (N/mm <sup>3</sup> )	Mode II $k_x$ (N/mm <sup>3</sup> )
1	41.0	104.6
2	112.7	203.7
3	101.8	634.5
Average values	85.2	314.3

The experimental results have enabled also the estimation of the critical energy release rates in fracture modes I and II. Table 2 summarises the values computed through Eqs. (9), according to the EBT and SBT models (respectively, with and without the crack length correction parameters). The SBT model appears to underestimate significantly the critical energy release rate with respect to the EBT model, as documented directly by the experimental results. Please, notice that the  $G_{Ic}$  values are average values calculated from the applied loads and corresponding delamination lengths recorded during crack propagation (see Fig. 5). Instead, the  $G_{IIc}$  values are single values obtained from the applied load and delamination length at the onset of crack propagation.

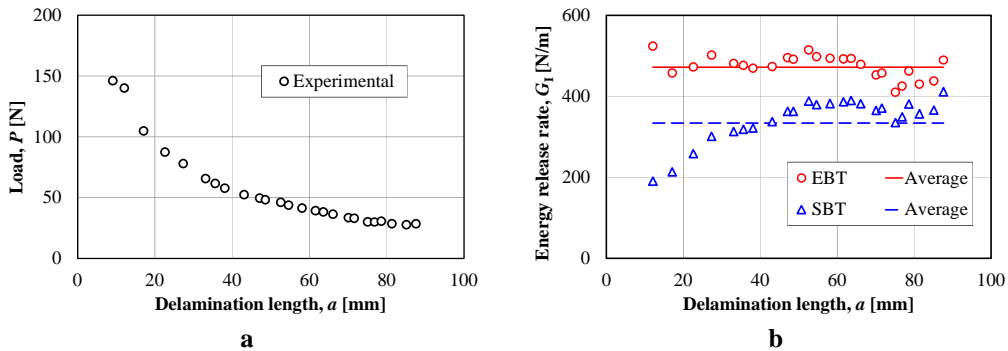


Figure 5: Determination of  $G_{Ic}$ : a) applied load vs. delamination length; b) energy release rate vs. delamination length.

Table 2: Critical energy release rates.

Specimen No.	Mode I		Mode II	
	$G_{Ic}^{SBT}$ (J/m <sup>2</sup> )	$G_{Ic}^{EBT}$ (J/m <sup>2</sup> )	$G_{IIc}^{SBT}$ (J/m <sup>2</sup> )	$G_{IIc}^{EBT}$ (J/m <sup>2</sup> )
1	220.2	335.8	447.6	1295.6
2	426.7	603.6	569.8	1271.1
3	333.6	471.6	516.1	841.5
Average values	326.9	470.3	511.2	1136.1

## 5 CONCLUSIONS

We have illustrated an experimental compliance calibration strategy, which enables the estimation of the elastic interface constants to be used when modelling delaminated laminates as assemblages of sublaminates connected by elastic interfaces.

The method is based on the analytical solution for an enhanced beam-theory model of the MMB test, derived in a previous study. Here, a nonlinear least squares fitting procedure has been applied to obtain the values of the elastic interface constants from the experimental results of DCB and ENF tests.

Preliminary experimental tests have been conducted, offering a first confirmation of the effectiveness of the proposed strategy. Further extensive experimental tests and numerical simulations are required to validate the method fully. Some aspects, such as the effects of geometric nonlinearities, deserve further investigation from the theoretical point of view.

## ACKNOWLEDGEMENTS

The authors wish to thank Alessandra Passaro and Antonella Tarzia of the CETMA consortium for their valuable support in conducting the experimental tests.

The financial support of the Italian Ministry of Education, University and Research (MIUR) under programme PRIN 2008 “Light structures based on multiscale material in civil engineering: stiffness and strength, assembly and industrial repeatability” (Prot. N. 20089RJKYN\_002) is gratefully acknowledged.

## References

- [1] Tay, T.E., “Characterization and analysis of delamination fracture in composites: An overview of developments from 1990 to 2001”, *Appl. Mech. Rev.*, **56**(1), 1–31 (2003).
- [2] Friedrich, K, (editor), *Application of Fracture Mechanics to Composite Materials*, Elsevier, Amsterdam (1989).
- [3] Adams, D.F., Carlsson, L.A. and Pipes, R.B., *Experimental Characterization of Advanced Composite Materials*, 3rd edition, CRC Press, Boca Raton (2003).
- [4] ASTM, *Standard Test Method for Mixed Mode I-Mode II Interlaminar Fracture Toughness of Unidirectional Fiber Reinforced Polymer Matrix Composites*, D6671/D6671M-06, American Society for Testing and Materials, West Conshohocken (2006).
- [5] AECMA, *Determination of interlaminar fracture toughness energy. Mode I –  $G_{Ic}$* , prEN 6033:1995, European Association of Aerospace Industries, Bruxelles (1995).
- [6] AECMA, *Determination of interlaminar fracture toughness energy. Mode II –  $G_{IIc}$* , prEN 6034:1995, European Association of Aerospace Industries, Bruxelles (1995).

- [7] Allix, O. and Ladevèze, P., “Interlaminar interface modelling for the prediction of delamination”, *Compos. Struct.*, **22**(4), 235–242 (1992).
- [8] Bennati, S., Colleluori, M., Corigliano, D. and Valvo, P.S., “An enhanced beam-theory model of the asymmetric double cantilever beam (ADCB) test for composite laminates”, *Compos. Sci. Technol.*, **69**(11-12), 1735–1745 (2009).
- [9] Bennati, S., Fiscaro, P. and Valvo, P.S., “An enhanced beam-theory model of the mixed-mode bending (MMB) test – Part I: literature review and mechanical model”, *Meccanica*, **48**(2), 443–462 (2013).
- [10] Bennati, S., Fiscaro, P. and Valvo, P.S., “An enhanced beam-theory model of the mixed-mode bending (MMB) test – Part II: applications and results”, *Meccanica*, **48**(2), 465–484 (2013).
- [11] Vannucci, P. and Verchery, G., “A special class of uncoupled and quasi-homogeneous laminates”, *Compos. Sci. Technol.*, **61**(10), 1465–1473 (2001).
- [12] Jones, R.M., *Mechanics of composite materials*, 2nd edition. Taylor & Francis Inc., Philadelphia (1999).
- [13] Williams, J.G., “End corrections for orthotropic DCB specimens”, *Compos. Sci. Technol.*, **35**(4), 367–376 (1989).
- [14] Wang, Y. and Williams, J.G., “Corrections for mode II fracture toughness specimens of composites materials”, *Compos. Sci. Technol.*, **43**(3), 251–256(1992).